IOP Publishing Journal of Micromechanics and Microengineering
J. Micromech. Microeng. **25** (2015) 115021 (9pp) doi:10.1088/0960-1317/25/11/115021

Performance enhancement on a micro-column structure reformer via thick-film photoresist pre-protection

Kuo-Yang Huang[1], Shu-Ping Lai[1], Hsueh-Sheng Wang[1], Fan-Gang Tseng[1] and Yuh-Jeen Huang[2]

[1] Department of Engineering and System Science, National Tsing Hua University, Hsinchu, Taiwan
[2] Department of Biomedical Engineering and Environmental Sciences, National Tsing Hua University, Hsinchu 30013, Taiwan

E-mail: yjhuang@mx.nthu.edu.tw and fangang@ess.nthu.edu.tw

Received 17 March 2015, revised 27 August 2015
Accepted for publication 3 September 2015
Published 12 October 2015

Abstract

In this study, a reformer stack was made by incorporating silicon technology into catalyst preparation. The volumes of an individual micro-channel chip and a whole reformer stack were 0.4 cm^3 and 16 cm^3, respectively. Different weight ratios (B/C = 35, 15, 5, and 0 wt%) of binder (a mixture of boehmite, bentonite, and deionized water) and catalyst were mixed to find out the optimal adhesion between the catalyst and silicon substrate. The results from this study show that the percentage of weight loss of the catalyst on the silicon substrate increases as the concentration of inorganic binder decreases. To further increase the exposed surface area of the catalyst deposited on the micro-channels, micro-column structures were integrated into the channels; however, a blockage of the catalysts among the columns during deposition was encountered. To resolve this issue, a method of pre-protecting the micro-channel with thick-film photoresist was utilized for the catalyst deposition, and the performance of the fabricated micro-column reformer was able to reach a 95% methanol conversion rate, 90% hydrogen selectivity, and 1.6×10^{-5} (mol min^{-1}) hydrogen yield at 225 °C in the partial oxidation of methanol reaction.

Keywords: partial oxidation of methanol (POM), micro-channel reformer, catalyst coating, thick film photoresist

(Some figures may appear in colour only in the online journal)

1. Introduction

Nowadays, fossil fuels such as coal, petroleum, and natural gas are heavily depended upon for global energy supplies. However, many negative effects from the heavy utilization of fossil fuels have been encountered for decades such as water pollution, acid rain, global climate change, and respiratory diseases. Moreover, low-priced fossil fuels from the Earth's natural resources will only last for a limited number of years [1]. Therefore, finding a clean and efficient energy source that can substitute fossil fuels has become a crucial issue. Renewable energies such as solar power, wind power, water power, terrestrial heat, and biomass energy are potential ways to solve energy deficiency and environmental pollution problems. However, the reliability of a sufficient energy supply from these renewable energies is still an issue. In recent years, fuel cells have become potential alternative energy resources due to their advantages of high efficiency, low contamination, and nearly no noise generation [2–5]. Reforming liquid-type fuel into hydrogen for high performance fuel cell operation is one of the more rational ways available to ease the challenges of the fuel carrying/transportation issue.

Four major reactions including methanol decomposition (MD), steam reforming of methanol (SRM), partial oxidation of methanol (POM), and partial oxidation and steam reforming of methanol (OSRM) have been developed for methanol

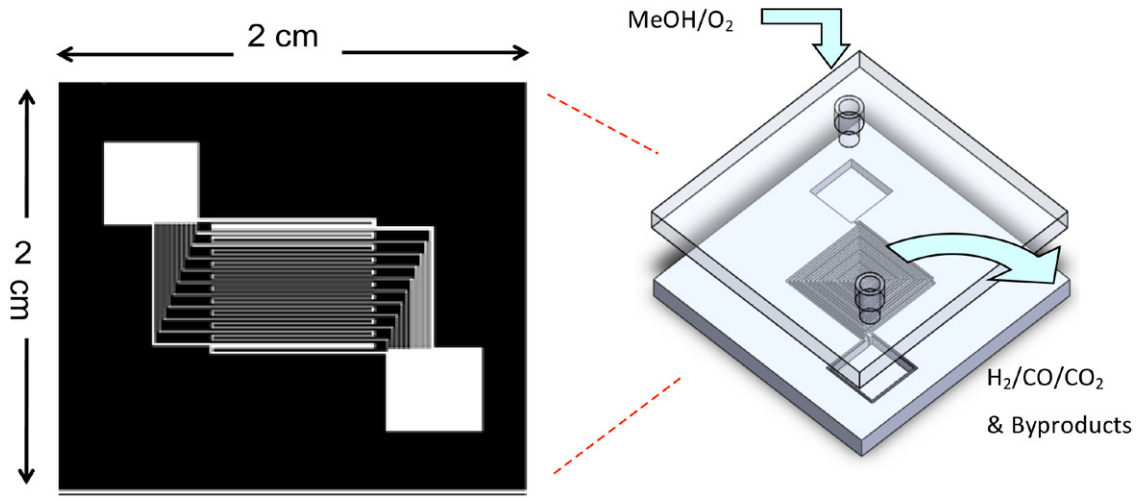

Figure 1. Micro-channel chip and its pattern.

reformation. Among them, SRM is the most frequently used [6, 7]. Stoichiometrically, one mole of methanol can produce 3 moles of hydrogen in SRM, but can produce only 2 moles of hydrogen in POM. However, POM, an exothermic reaction, has the advantages of producing less heat, a short start-up time, and can reach steady-state quickly. POM can be considered as an alternative choice for high-performance methanol reforming processes, even though its hydrogen generation rate is not as high as SRM. Besides, the POM reaction uses oxygen as the reactant gas, which makes the reaction much simpler than OSRM [8–12].

In a micro-channel system, micro-reactors are usually made of nonporous materials such as silicon wafer and glass [13–16]. However, coating catalysts onto such substances is difficult. High-quality coatings ensure that the catalysts can withstand high temperature without peeling off. Generally, particle size, solvent viscosity, solid content in the solvent, and concentration of the binder are all important factors that can determine the adhesion and uniformity of the coating. Mirodatos *et al* [17] studied the effects of viscosity, deposition time, particle size, and pH on the adhesion of catalyst coating. They were able to obtain films at a desired thickness of 25 μm with good adhesion and reasonable uniformity at the same time. Germani *et al* [18] researched the correlations between binder preparation parameters, coating properties, and catalyst activity in water gas shift reactions, and reported that molecular structure and weight would affect the viscosity of the solvent, the adhesion of the coating, and catalyst activity, respectively. Using syringes to coat a catalyst is a convenient way to perform catalyst deposition at lab scale with good layer quality [19, 20]. Datye *et al* used a gas-displacement technique to generate wall coatings of catalyst slurries in fused silica capillaries and ceramic microreactors, and then studied the effects of channel diameters, channel numbers, and the flow rates of gas and liquid on the coating amount and uniformity. The results showed that the inherent compact design of multi-channeled micro-reactors led to a higher possibility of successfully loading catalysts than a single channel with the same total reactor length. They also pointed out that it is important to keep relatively thick coatings from drying stresses in order to prevent cracking and loss of cohesion [21, 22]. The application of multi-channel benefits to lower the drop pressure of the reformer, and to avoid the adverse effects of inertia on the quality of the coated layer, and thus lead to a plug-free channel whereby all of the loaded catalyst is expected to be accessible for the reforming action [21, 23].

The goal of this study is to uniformly coat a Cu–Mn–Zn catalyst onto the inside walls of silicon micro-channels, to avoid the catalysts peeling off or the micro-channels clogging, and to optimize the performance in these reformers. In this paper, we report methods to coat a Cu–Mn–Zn-based catalyst solution prepared via the slurry method onto micro-channels. In addition, in order to enhance performance, micro-column structures were designed into channels to increase the exposed surface area and the loading amount of the catalyst. Moreover, a micro-channel reformer with catalyst preparation by thick-film photolithography was also proposed to improve catalyst loading.

2. Experiment

2.1. Fabrication of micro-channels

In this experiment, silicon wafer and Pyrex glass were chosen as the housing materials for the micro-channel reactors due to their strong resistance to high temperature during the methanol reforming reaction and good manufacturing capability for micro-machining and wafer bonding processes.

A multi-inlet, micro-channel pattern was designed and is shown in figure 1. We used a photolithography process to define the channel patterns, and utilized a laser cutting technique to make holes in the Pyrex glass for the inlet and outlet gases to flow through. To ensure tight connections between the Pyrex glass and silicon wafer and to avoid leakage of the reactant gases, an anodic bonding technique was used to bind the Pyrex glass and silicon wafer together. However, anodic bonding could only be conducted under extremely clean conditions. Therefore, without special protection, the catalyst could only be coated onto the micro-channels by the fill-and-dry

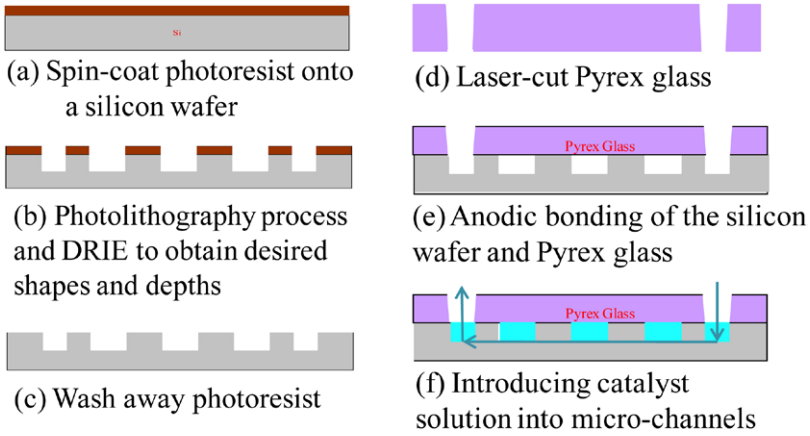

Figure 2. Flow chart of the micro-channel fabrication.

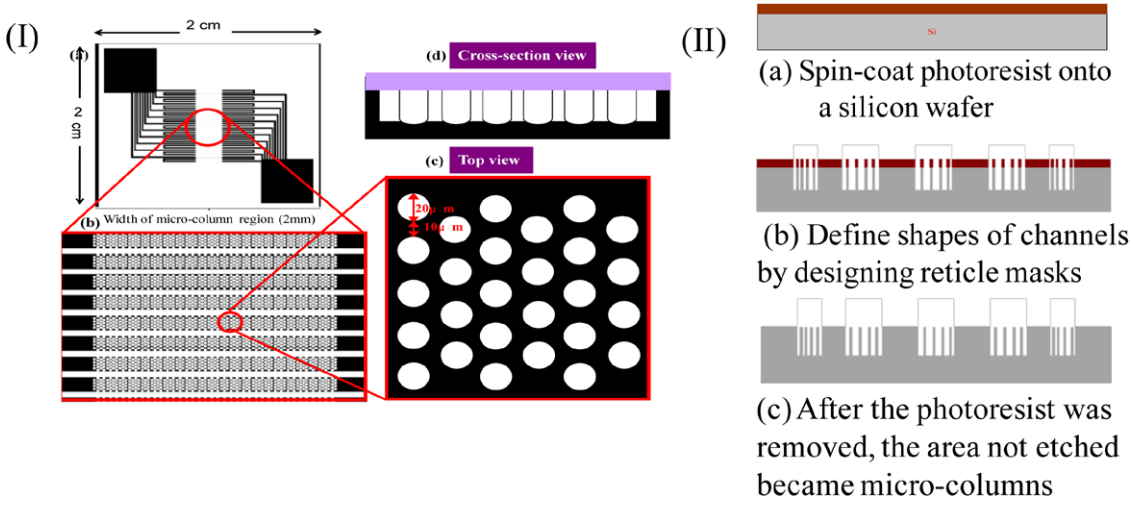

Figure 3. (I) Design of the micro-columns in the channels, (II) flow chart of the micro-column fabrication.

method after the anodic bonding was performed. The volume of each micro-channel chip is 2 cm × 2 cm × 0.1 cm, as shown in figure 1. Our micro-reactor consists of 11 capillaries, and each capillary is roughly 15 mm in length and 150 μm in width. A multi-inlet was designed to enhance the reaction area of the catalyst to the reactant gases, and also to make the catalyst loading easier. The winding path of each channel was fabricated in an attempt to increase the reaction time of the reactant gases and catalysts.

2.2. Fabrication of micro-reformers

2.2.1. Micro-channels. To fabricate micro-channels, a photoresist (AZ 9260) was first spin-coated onto a silicon wafer (figure 2). Secondly, by using a photolithography process and deep reactive ion etching (DRIE), the desired shapes and depths on the silicon wafer were obtained (b). Then the photoresist was stripped away (c). Next, the anodic bonding technique was employed to bind the Pyrex glass and the silicon substrates together (d), (e). Finally, catalyst solutions were introduced into the micro-channels (f). After the micro-channels had been dried in an oven at 100 °C overnight and calcined at 400 °C for 4 h to remove unwanted organic materials, the fabrication was complete.

2.2.2. Micro-channels with micro-columns. To increase the exposed surface area of the catalyst, micro-columns inside the channels were constructed. By designing patterns of photomasks, the widths and numbers of the micro-columns can be controlled. Figure 3(I) illustrates the micro-columns.

The fabrication of micro-columns also requires a photolithography process to define the patterns of the channels (figure 3(II)). The only difference is in the changes in the patterns of the photomasks (b). Areas not exposed to UV light would not be etched by DRIE, and thus become the structures of micro-columns (c). The width of each column was 20 μm, and the distance between the columns was 10 μm.

2.2.3. Micro-channels with thick-film photolithography. In order to further improve and increase the loading of catalysts, an alternative way of catalyst deposition was developed and utilized in the channels equipped with micro-columns.

In contrast to the traditional way of coating catalysts using syringes, a thick-film photoresist was incorporated into this study as a sacrificial layer to protect the surface of the silicon wafer for catalyst loading in parallel. Catalysts can be loaded directly onto the surface of channels before anodic bonding. A flow chart of this process is shown in figure 4. First of all, a silicon wafer was spin-coated with photoresist, as shown in

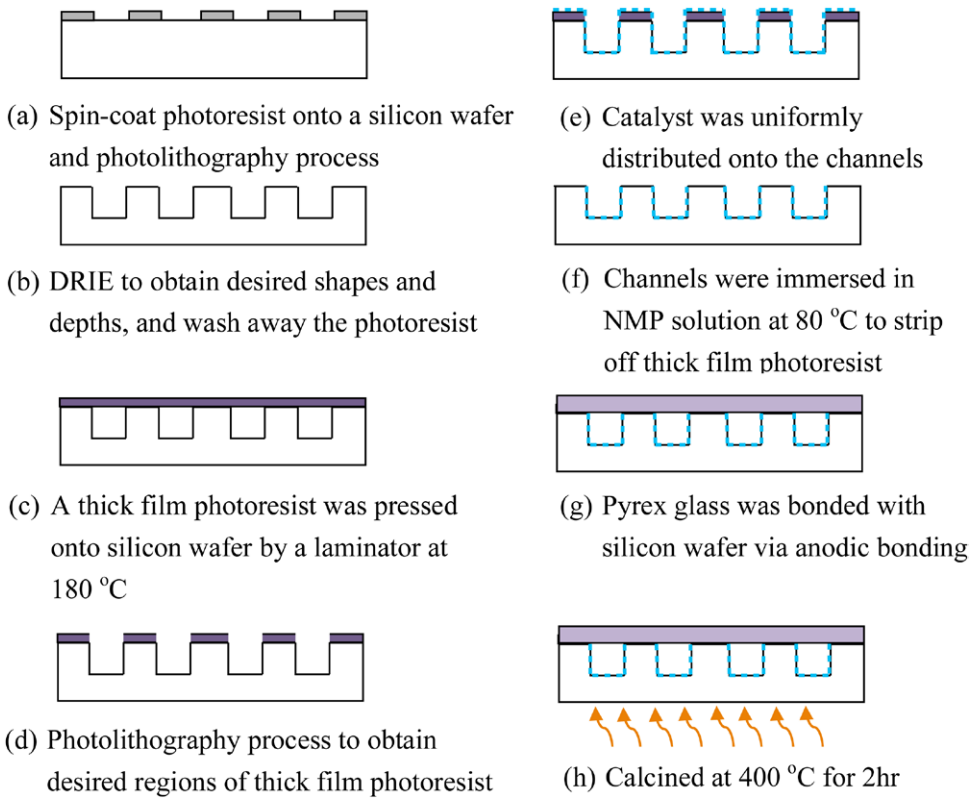

Figure 4. Flow chart of the thick-film coating process.

(a). Photolithography and DRIE processes were performed to obtain the desired shapes and depths of the channels. Then the photoresist was stripped away (b). A thick dry-film photoresist was then pressed onto the wafer at 180 °C by a laminator (c). The photolithography process was once again performed to obtain the desired regions of the thick-film photoresist (d). Next, the catalyst was uniformly distributed onto the channels (e). The thick-film photoresist was used as a sacrificial layer to protect the top surface of the silicon wafer. After coating the catalysts onto the silicon wafer, it was immersed in N-Methyl-2-pyrrolidone (NMP) solution at 80 °C to strip off the thick-film photoresist (f). Finally, the Pyrex glass could be successfully bonded with the silicon wafer (g). After calcination at 400 °C for 2 h, the process was complete.

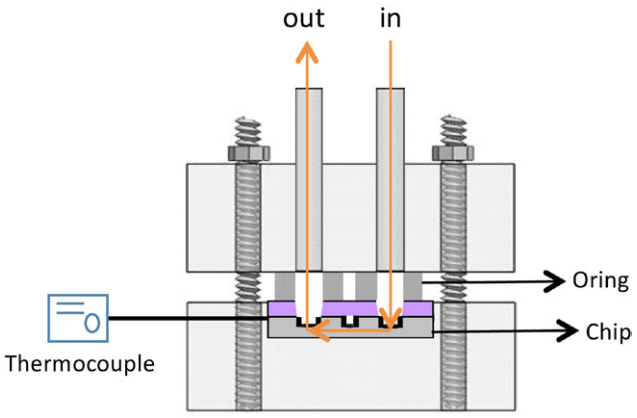

Figure 5. Schematic of the micro-reactor.

2.3. Assembly of micro-reactors

Since the activity tests of micro-reactors in the methanol reforming reaction had to be operated at about 250 °C, all wires connected to the reaction units must be made of materials that resist high temperature. Also, the gas tightness should be taken into account to avoid gas leakage. A schematic of the micro-reactor is shown in figure 5. For assembling the micro-reactor, one micro-channel chip was placed in the center between two stainless steel plates. The holders were designed to have one inlet and one outlet tube that allow the reactant gases to flow in and out. Two high-temperature-resistant O-rings were used to prevent the gases from leaking out. The temperature was controlled via a hot plate under this micro-channel reactor set. A thermocouple detector was placed through the stainless steel holder to measure the actual reaction temperature of each micro-channel chip unit.

2.4. Catalyst preparation

A $Cu_{30}Mn_{20}ZnO$ catalyst was prepared via co-precipitation methods and a detailed procedure is described in [24]. All the precursor salts, such as copper nitrate ($Cu(NO_3)_2{\cdot}2.5H_2O$), zinc nitrate ($Zn(NO_3)_2{\cdot}6H_2O$), and manganese nitrate ($Mn(NO_3){\cdot}4H_2O$) were nitrate salts. The atomic ratio of Cu/Mn/Zn was 3 : 2 : 5. A catalyst slurry was prepared by mixing the fresh catalyst with an alumina binder [boehmite (Remet), bentonite (Sigma)] at the 35, 15, 5, 0 wt% of binders to catalysts (B/C) into deionized water. The slurries were stirred with ultrasound treatment for 4 h to uniformly disperse the

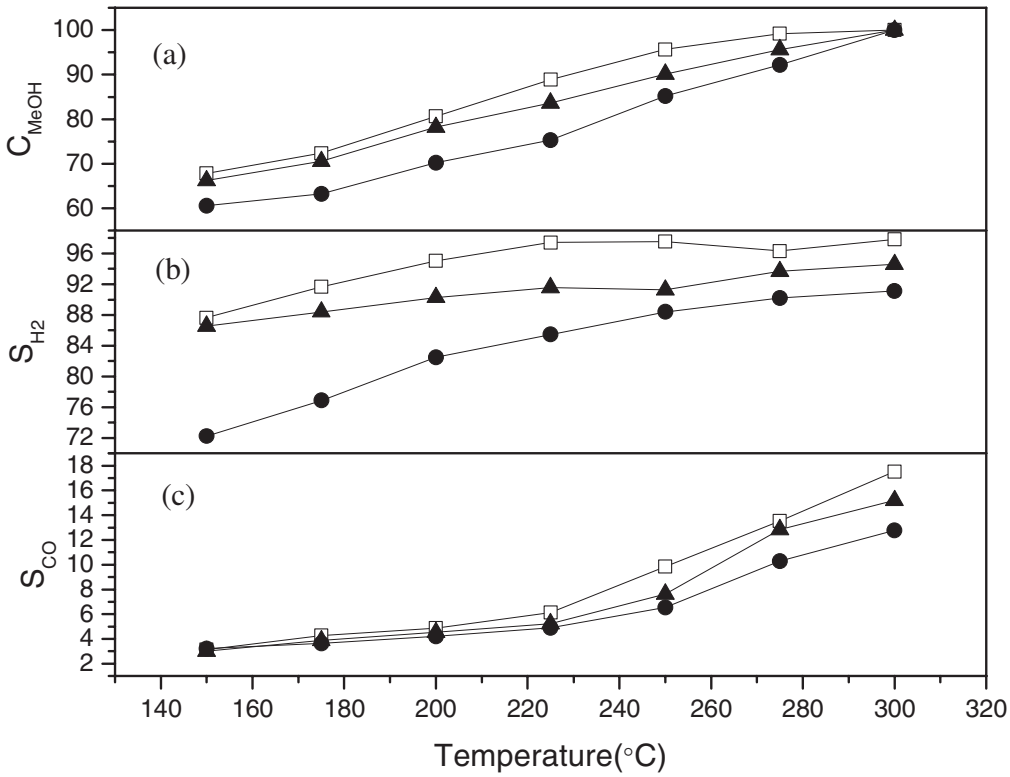

Figure 6. Temperature profiles of the catalytic performance: (a) conversion of methanol (C_{MeOH}), (b) selectivity of hydrogen (S_{H_2}), and (c) selectivity of carbon monoxide (S_{CO}), over (□) $Cu_{30}Mn_{20}ZnO$, (▲) $Cu_{30}Mn_{20}ZnO$ B/C = 5 wt%, (●) $Cu_{30}Mn_{20}ZnO$ B/C = 15 wt%, during the POM reaction in a fixed-bed reactor.

particles in the solution before being introduced into the micro-channel chip.

2.5. The adhesive strength test

The adhesive strength of slurries on a silicon chip was estimated by an ultrasonic vibration test. The slurry was dropped onto the chip surface and dried at 60 °C overnight. After drying, the slurry-coated chip was calcined at 400 °C for 2 h. Then the chip was placed in DI water under 135 W of ultrasonic vibration for 30 min. The fraction of weight loss (F_L) of the catalyst was calculated as follows:

$$F_L = \frac{W - W_L}{W} \times 100\%$$

where F_L is the fraction of weight loss during ultrasonic treatment, W is the load amount of catalyst before treatment and W_L is the load after treatment.

2.6. Experimental set-up and performance characterization

A micro-channel chip was first placed in a stainless steel holder, then the slurry solution of the catalyst was injected into the channels through the tubes on the stainless holder by syringes. Next, this micro-channel chip was dried in an oven at 105 °C overnight, and was later calcined at 400 °C for 2 h. Before proceeding to the micro-reactor performance tests, each micro-channel chip had to be placed in the holder to run the gas-tightness test. Nitrogen gas was vented to the reactor stack, and this whole stack was immersed in water to check if any gas was leaking out.

The reactant gases were methanol (12.2%) and oxygen (6.1%), and nitrogen (81.7%) was used as a carrier gas. The total flow rate of the reactant gases was set at 2 ml min^{-1}. Product analysis was done by a TCD-GC equipped with columns, Porapak Q (used to detect MeOH, CO_2 and H_2O), and Molecular Sieve 5A (used to detect CO, O_2, and H_2). The major products found in the performed reactions were H_2, CO_2, CO, and H_2O (found in POM). The conversion rate of methanol (C_{MeOH}), hydrogen selectivity (S_{H_2}), hydrogen yield (Y_{H_2}), and CO selectivity (S_{CO}) are generally defined as:

$$C_{MeOH} = (n_{MeOH,in} - n_{MeOH,out})/n_{MeOH,in} \times 100\%$$

$$S_{H_2} = n_{H_2}/(n_{H_2O} + n_{H_2}) \times 100\%$$

$$Y_{H_2} = n_{H_2}\ min^{-1}$$

$$S_{CO} = n_{CO}/(n_{CO_2} + n_{CO}) \times 100\%.$$

3. Results and discussion

3.1. Catalysis activity of fixed-bed under POM reaction

Figure 6 shows the temperature profiles of the catalytic performance over $Cu_{30}Mn_{20}ZnO$ B/C = x wt% catalysts in a fixed-bed reactor. The methanol conversion was increased as the reaction temperature (T_R) increased in the POM reaction. However, the addition of a binder would decrease the reaction conversion. When the percentage of binder (B/C) was 15 wt%, C_{MeOH} and S_{H_2} were reduced; i.e. from 98% and

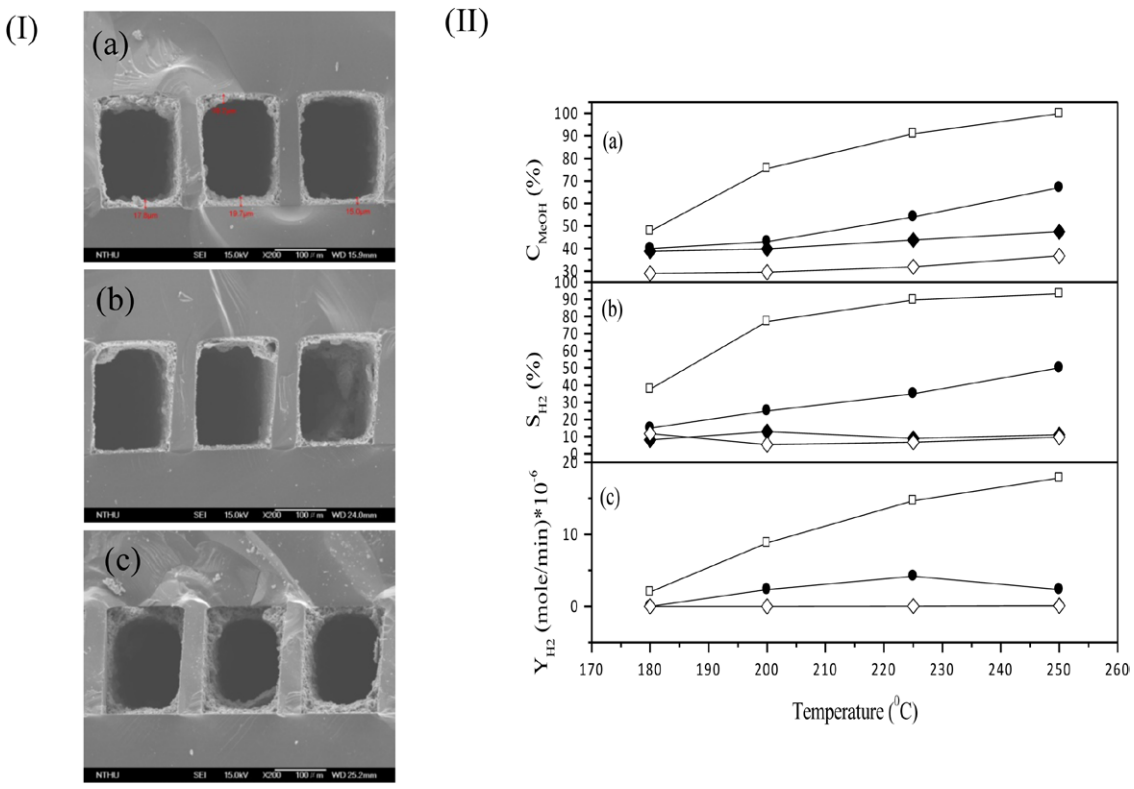

Figure 7. (I) SEM images (side view) of micro-channels loaded with slurries of different binders to catalyst weight ratios (B/C wt%): (a) 15 wt% (b) 5 wt% and (c) 0 wt%. (II) Temperature profiles of catalytic performance: (a) conversion of methanol (C_{MeOH}), (b) selectivity of hydrogen (S_{H_2}), (c) yield of hydrogen (Y_{H_2}), over (□) $Cu_{30}Mn_{20}ZnO$, (●) $Cu_{30}Mn_{20}ZnO$ B/C = 15 wt%, (♦) $Cu_{30}Mn_{20}ZnO$ B/C = 35 wt% during the POM reaction in micro-reformers, and over (◊) $Cu_{30}Mn_{20}ZnO$ B/C = 35 wt% during the POM reaction in micro-reformers with 2 mm regions of micro-columns.

97% to 75% and 85%, respectively, at 225 °C. We supposed that most of the catalyst particles were covered with aluminum oxides, reducing the active surface sites exposed to the reactants, thus resulting in the worst performance.

3.2. Effect of binder amount

Under strong ultrasonic vibration (135 W) for 30 min, we observed that the adhesion increased with increasing the binder ratio. The weight loss of the binder/catalyst (B/C) weight ratios of 35 wt%, 15 wt%, and 5 wt% were 23%, 82%, and 96%, respectively. The optimum ratio for the best adhesion was at about 50 wt% of B/C and the weight loss was less than 10%.

3.2.1. SEM morphology of the catalyst. Figure 7(I) shows the SEM images of the channels after repetitive loading of the slurry solution with 15 wt%, 5 wt%, and 0 wt% of binder/catalyst (B/C) weight ratios, respectively. We can clearly observe that the catalyst was uniformly distributed onto the micro-channels, forming a catalyst layer deposited onto the surface of the micro-channels. For B/C = 0 wt%, we found that even without the binder, the catalyst could still be coated well on the channels. With the same times of repetitive loading of slurry solutions at B/C = 0 wt%, which had the highest concentration of catalyst, a compact catalyst layer could accumulate, reaching an average thickness of 25 μm. On the other hand, although the inorganic binder enhanced the adhesion between the catalyst and silicon substrate, the concentration of the catalyst in the slurry was relatively lower. In addition, due to the accumulation of the catalyst with the binder, some catalyst may block the entrance of channel and lead to uniform coating. The thickness of the deposited catalysts with B/C = 15 wt% and 5 wt% were 17 μm and 22 μm, respectively, and both of them were thinner than the layer of B/C = 0 wt%. Table 1 lists the total catalyst amount of each channel detected by inductively coupled plasma-mass spectrometry. With the increment of B/C, the loading amount of the catalyst decreased.

Table 1. Total catalyst amounts in the channels.

B/C (wt%)	Coating method	Micro-column region (mm)	Total catalyst amount (μg)
0	Thick film	None	3383
		1	4888
0	Syringe	None	2797
5		None	2567
15		None	1089
35		None	598
		2	631

3.2.2. Activity tests of micro-reformers. The activity test of catalysts in a micro-reformer is shown in figure 7(II). The catalyst without binder exhibited the highest activity. At 200

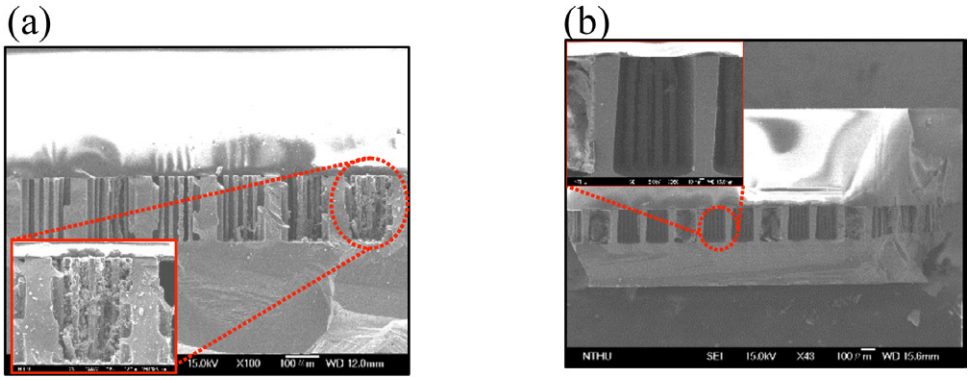

Figure 8. Cross-section views of the micro-channels with micro-columns (a) clogged and (b) unclogged with the catalyst.

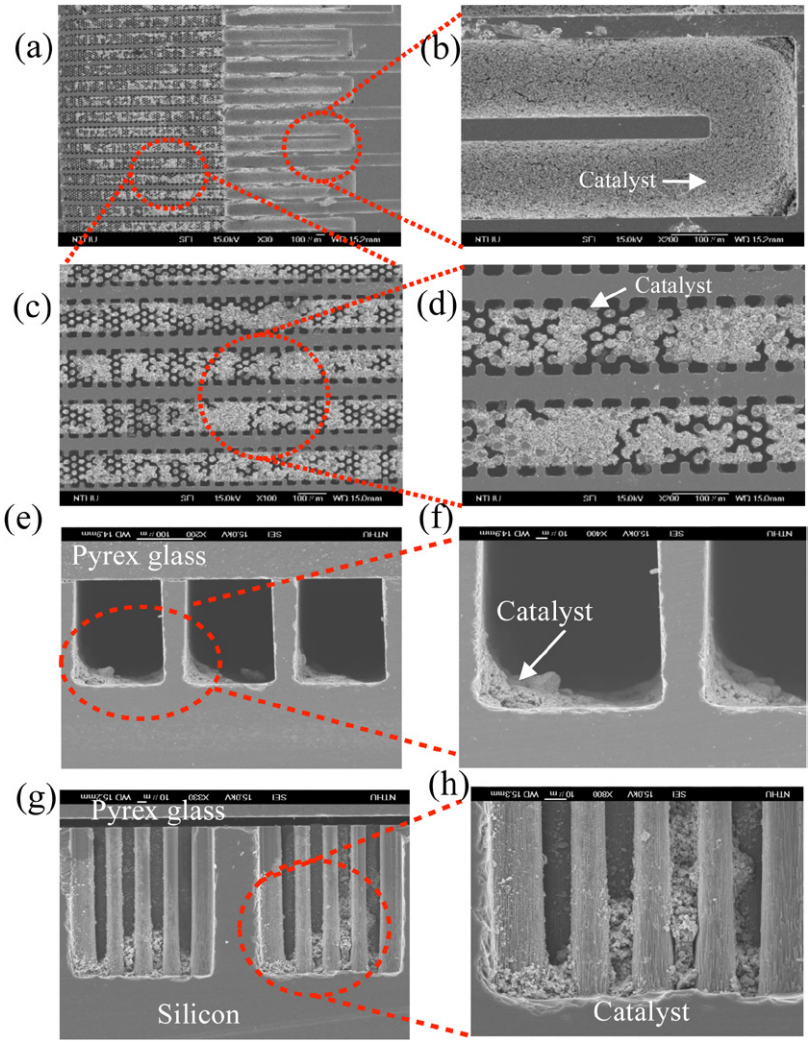

Figure 9. SEM images of the top views of the channels with micro-columns loaded with a catalyst via a thick-film coating process. (a) Channels w/wo micro-columns, (b) channels without micro-columns, (c) micro-column structures loaded with a catalyst, (d) enlargement of (c) and SEM images of the cross-section views of (e) micro-channels without micro-columns, (f) enlargement of (e), (g) micro-channels with micro-columns, (h) enlargement of (g).

°C, its methanol conversion rate could reach approximately 75%, whereas B/C = 15 wt% and 35 wt% had only 43% and 39%, respectively. In addition, the hydrogen selectivity was lowered from 80% to 15% by increasing the B/C to 35 wt%. Despite the fact that the addition of a binder to the catalyst slurry was to enhance the adhesion between the catalyst and silicon substrate, large amounts of binder would not only lower the concentration of the catalyst in the slurry solution, but also lower the efficiency of the catalyst. This consequently resulted in the worst catalytic performance in micro-reformers.

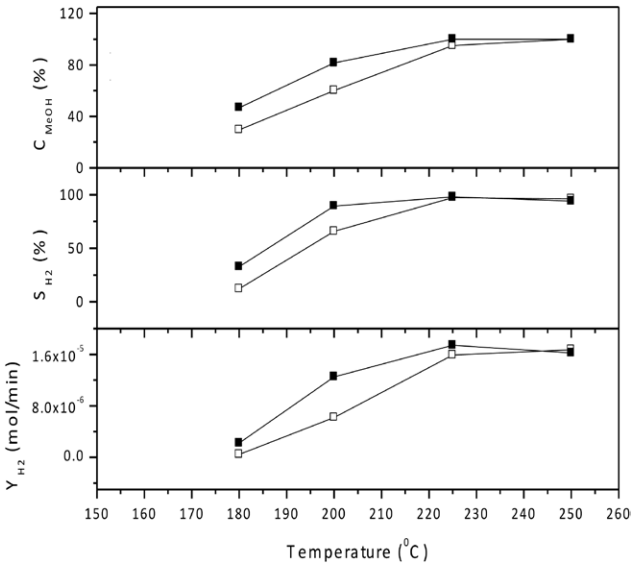

Figure 10. Activity tests of $Cu_{30}Mn_{20}ZnO$ during the POM reaction via the thick-film coating process in micro-reformers with (■) and without (□) 1 mm regions of micro-columns.

3.3. Micro-columns to increase the catalyst reaction area

Although repetitive loading of the slurry solution can increase the amount of catalyst on the micro-channels, these heavy and compact catalyst layers might block the diffusion of the reactant gases. To solve this issue, micro-column structures combined with channels were designed and integrated into micro-channels.

With these micro-column structures, the catalyst could be uniformly distributed onto micro-channels and thus more reaction areas were created. The activity test results of $Cu_{30}Mn_{20}ZnO$ B/C = 35 wt% via the syringe coating method in the reformers w/wo 2 mm regions of micro-columns are shown in figure 7(II). Nonetheless, instead of having an improved performance, the methanol conversion rate and hydrogen yield of the channels with micro-column structures were lower than anticipated. In addition, the total catalyst amounts ($Cu_{30}Mn_{20}ZnO$ B/C = 35 wt%) in both channels (w/wo 2 mm regions of micro-columns) were nearly the same (table 1). Figures 8(a) and (b) are cross-section views of the channels with micro-column structures after the catalyst was coated by syringes. It can be clearly observed in figure 8(a) that the catalysts are mostly clogged in some parts of the micro-columns, whereas in figure 8(b), some micro-columns are not completely or evenly coated with any catalyst. Because the catalyst solutions were directly injected into the channels through the inlet and outlet holes during the coating process, the narrow space between the micro-columns probably intercepted the catalysts, resulting in tunnel blockage; thus, the non-uniform deposition of the catalyst was observed. This phenomenon led to poor performance. To solve the clogging issue, instead of using syringes to pump the slurry serially through the micro-channel, a new method by directly depositing the catalyst onto the whole micro-channel surface in parallel before wafer binding was proposed. To prevent the contamination of slurries on the unbound silicon wafer surface, dry thick-film lithography was employed.

3.4. Thick-film photolithography process

By using dry thick-film lithography, the catalysts can be loaded directly and more uniformly onto the surface of channels before anodic bonding. Figures 9(a)–(h) show the top views and cross-section images of the micro-channels consisting of micro-columns loaded with a catalyst via a thick-film photolithography process. Not the same as the traditional way of coating catalysts using syringes, the catalysts were successfully distributed onto the regions w/wo micro-columns. Figures 9(e)–(h) show the cross-section images of the micro-channels w/wo micro-columns, and the Pyrex glass was combined with silicon substrate. This shows that this process is viable for catalyst distribution and glass bonding.

3.4.1. Activity tests of the improved micro-reformers. The activity tests of reformers w/wo 1 mm regions of micro-columns via the thick-film process are shown in figure 10. The results show that with more catalyst loaded onto the micro-channels, the methanol conversion rate and hydrogen yield were enhanced. The surface area in a plain micro-channel chip is 2.46×10^{-4} m^2, whereas it is 3.06×10^{-4} m^2 in micro-columns. The overall increase in surface area is 1.24 times after using the micro-column structures. The catalyst amount increased ca. 1.44 times (shown in table 1). Thus, the expected performance should be enhanced ca. $1.44 \times 1.24 = 1.79$ times. At 200 °C, micro-channels with 1 mm lengths of regions of the micro-column structure via thick-film coating had the higher performance and the methanol conversion can be improved ca. 1.8 times, which is quite consistent with what was expected. Moreover, at higher temperature, nearly 100% of C_{MeOH} and S_{H_2} can be reached in micro-reformers w/wo micro-columns, which means the amount of the catalysts is enough for the reactants to undergo a complete reaction. In this micro-reformer with 1 mm regions of micro-columns, the optimum operation condition is at 225 °C, and the methanol conversion rate, hydrogen selectivity, and hydrogen yields are 95%, 90%, and 1.6×10^{-5} mol min^{-1}, respectively.

The results shown in figure 10 indicate that the micro-column structures have been successfully installed onto micro-channels, the obstacles of introducing the catalyst to micro-columns have been overcome, and the performance of the micro-reformers has been enhanced by utilizing thick-film photolithography. The use of thick-film photoresist enables the process of catalyst loading before the Pyrex glass and silicon bonding. In the micro-fabrication/micro-reactor field, this can be applied to all other bonding processes that require a clean surface on both sides when attempting to load a large amount of substance uniformly onto the silicon substrate.

4. Conclusions

In this study, silicon etching, anodic bonding, micro-columns, and a new coating method (thick-film photolithography) were applied to enhance the performance of micro-reformers. An average 25 μm thickness of catalyst layer was achieved after repetitive loading of a catalyst solution.

Moreover, the existence of a micro-column structure, the original design of which is to enhance the exposure surface of the catalyst, might stop the slurry and lead to a non-uniform distribution of the catalyst and poor performance of the micro-reformers.

Through thick-film photolithography, we can overcome the clogging problem, increase the catalyst loading amount, and thus enhance the micro-reformer performance. We improved the micro-reactor performance and reached a 95% methanol conversion rate, 90% hydrogen selectivity, and 1.6×10^{-5} (mol min^{-1}) hydrogen yield at 225 °C.

Acknowledgments

We would like to acknowledge the support from the Ministry of Science and Technology (Project Number: MOST 104-3113-E-007-002-).

References

[1] Charles B 1971 Purpose in the Universe: a search for wholeness *Zygon* **6** 4–27
[2] Acres G J K 2001 Recent advances in fuel cell technology and its applications *J. Power Sources* **100** 60–6
[3] McNicol B D, Rand D A J and Williams K R 2001 Fuel cells for road transportation purposes—yes or no *J. Power Source* **100** 47–89
[4] Cacciola G, Antonucci V and Freni S 2001 Technology update and new strategies on fuel cells *J. Power Sources* **100** 67–79
[5] Larminie J and Dicks A 2002 *Fuel Cell Systems Explained* (New York: Wiley) ch 1, pp 1–24
[6] Lindstrom B and Pettersson L J 2001 Hydrogen generation by steam reforming of methanol over copper-based catalysts for fuel cell applications *Int. J. Hydrog. Energy* **26** 923–33
[7] Takahashi T, Inoue M and Kai T 2001 Effect of metal composition on hydrogen selectivity in steam reforming of methanol over catalysts prepared form amorphous alloys *Appl. Catal.* A **218** 189–95
[8] Velu S, Suzuki K and Osaki T 1999 Selective production of hydrogen by partial oxidation of methanol over catalysts derived from CuZnAl-layered double hydroxides *Catal. Lett.* **62** 159–67
[9] Wang Z F, Xi J Y, Wang W P and Lu G X 2003 Selective production of hydrogen from partial oxidation of methanol over silver catalysts at low temperatures *J. Mol. Catal.* A **191** 123–36
[10] Cubeiro M L and Fierro J L G 1998 Selective production of hydrogen by partial oxidation of methanol over ZnO-supported palladium catalysts *Appl. Catal.* A **168** 307–22
[11] Schuyten S and Wolf E E 2006 Selective combinatorial studies on Ce and Zr promoted Cu/Zn/Pd catalysts for hydrogen production via methanol oxidative reforming *Catal. Lett.* **106** 7–14
[12] Mo L, Zheng X and Yeh C T 2004 Selective production of hydrogen from partial oxidation of methanol over silver catalysts at low temperatures *Chem. Commun.* **12** 1426–7
[13] Srinivas S, Dhingrab A, Imb H and Gulari E 2004 A scalable silicon microreactor for preferential CO oxidation: performance comparison with a tubular packed-bed microreactor *Appl. Catal.* A **274** 285–93
[14] Pattekar A V and Kothare M V 2004 A microreactor for hydrogen production in micro fuel cell applications *J. Microelectromech. Syst*. **13** 7
[15] Ajmera S K, Delattre C and Schmidt M A 2003 Microreactors for measuring catalyst activity and determining reaction kinetics *Sci. Technol. Catal.* **145** 97–102
[16] Kikutani Y, Hibara A, Uchiyama K, Hisamoto H, Tokeshi M and Kitamori T 2002 Pile-up glass microreactor *Lab Chip* **2** 193–6
[17] Stefanescu A, van Veen A C, Mirodatos C, Beziat J C and Duval-Brunel E 2007 Wall coating optimization for microchannel reactors *Catal. Today* **125** 16–23
[18] Germani G, Stefanescu A, Schuurman Y and van Veen A C 2007 Preparation and characterization of porous alumina-based catalyst coatings in microchannels *Chem. Eng. Sci.* **62** 5084–91
[19] Lim M S, Kim M R, Noh J and Woo S I 2005 A plate-type reactor coated with zirconia-sol and catalyst mixture for methanol steam-reforming *J. Power Sources* **140** 66–71
[20] Won J Y, Jun H K, Jeon M K and Woo S I 2006 Performance of microchannel reactor combined with combustor for methanol steam reforming *Catal. Today* **111** 158–63
[21] Conant T, Karim A and Datye A 2007 Coating of steam reforming catalysts in non-porous multi-channeled microreactors *Catal. Today* **125** 11–5
[22] Conant T, Karim A, Rogers S, Samms S, Randolph G and Datye A 2006 Wall coating behavior of catalysts slurries in non-porous ceramic microstructures *Chem. Eng. Sci.* **61** 5678–85
[23] Hsieh S S, Yang S H, Kuo J K, Huang C F and Tsai H H 2006 Study of operational parameters on the performance of micro PEMFCs with different flow fields *Energy Convers. Manag.* **47** 1868–78
[24] Huang H Y, Lee S H and Huang Y J 2015 Adhesion optimization for catalyst coating on silicon-based reformer *J. Adhes. Sci. Technol.* **29** 1937–50